AMB Express

ORIGINAL ARTICLE Open Access

Molecular docking and antimicrobial activities of photoexcited inhibitors in antimicrobial photodynamic therapy against *Enterococcus faecalis* biofilms in endodontic infections

Maryam Pourhajibagher[1], Zahra Javanmard[2] and Abbas Bahador[2,3,*]

Abstract
Antimicrobial photodynamic therapy (aPDT) is a promising approach to combat antibiotic resistance in endodontic infections. It eliminates residual bacteria from the root canal space and reduces the need for antibiotics. To enhance its effectiveness, an *in silico* and in vitro study was performed to investigate the potential of targeted aPDT using natural photosensitizers, Kojic acid and Parietin. This approach aims to inhibit the biofilm formation of *Enterococcus faecalis*, a frequent cause of endodontic infections, by targeting the Ace and Esp proteins. After determining the physicochemical characteristics of Ace and Esp proteins and model quality assessment, the molecular dynamic simulation was performed to recognize the structural variations. The stability and physical movement of the protein-ligand complexes were evaluated. *In silico* molecular docking was conducted, followed by ADME/Tox profiling, pharmacokinetics characteristics, and assessment of drug-likeness properties of the natural photosensitizers. The study also investigated the changes in the expression of genes (*esp* and *ace*) involved in *E. faecalis* biofilm formation. The results showed that both Kojic acid and Parietin complied with Lipinski's rule of five and exhibited drug-like properties. *In silico* analysis indicated stable complexes between Ace and Esp proteins and the natural photosensitizers. The molecular docking studies demonstrated good binding affinity. Additionally, the expression of the *ace* and *esp* genes was significantly downregulated in aPDT using Kojic acid and Parietin with blue light compared to the control group. This investigation concluded that Kojic acid and Parietin with drug-likeness could efficiently interact with Ace and Esp proteins with a strong binding affinity. Hence, natural photosensitizers-mediated aPDT can be considered a promising adjunctive treatment against endodontic infections.

Keywords *Enterococcus faecalis*, Kojic acid, Parietin, *In silico*, Antimicrobial photodynamic therapy, Endodontic infections

*Correspondence:
Abbas Bahador
abahador@sina.tums.ac.ir
[1]Dental Research Center, Dentistry Research Institute, Tehran University of Medical Sciences, Tehran, Iran
[2]Department of Microbiology, School of Medicine, Tehran University of Medical Sciences, Tehran, Iran
[3]Fellowship in Clinical Laboratory Sciences, BioHealth Lab, Tehran, Iran

Introduction

Enterococcus faecalis is a common cause of endodontic infections, which are infections of the dental pulp and the surrounding tissues (Alghamdi and Shakir 2020). Endodontic infections can be painful and can lead to serious complications if not treated promptly (Segura-Egea and Martín-González 2020). Studies have shown the prevalence of *E. faecalis* in root canal-treated teeth with persistent infections (Zoletti et al. 2011; Alghamdi and Shakir 2020). It is resistant to many commonly used antibiotics, complicating treatment efforts. Additionally, *E. faecalis* can survive in harsh conditions, such as the presence of blood or pus, and can remain in the root canal system for extended periods (Hollenbeck and Rice 2012).

The persistence of *E. faecalis* in the root canal system is largely due to its ability to form biofilms, which hinder the penetration of disinfectants and antibiotics, making it difficult to eradicate the bacteria (Alghamdi and Shakir 2020). Biofilm formation is a complex process that involves several genes, including the *esp* and *ace* genes (Francisco et al. 2021). The *esp* gene, known as Enterococcal surface protein, is located on a pathogenicity island and encodes a surface protein that mediates the initial attachment of *E. faecalis* to host tissues and abiotic surfaces. The Esp protein also contributes to bacterial aggregation and biofilm formation (Toledo-Arana et al. 2001). Similarly, the *ace* gene, which stands for Aggregation substance, plays a role in biofilm formation by *E. faecalis*. The Ace protein is a surface protein that promotes cell-to-cell aggregation, a crucial step in biofilm development (Francisco et al. 2021).

To effectively treat endodontic infections caused by *E. faecalis*, it is important to use a combination of mechanical and chemical techniques. Mechanical techniques focus on removing infected tissue from the root canal, while chemical methods utilize antimicrobial agents to eradicate the bacteria (Pereira et al. 2021). However, as previously mentioned, *E. faecalis* exhibits resistance to many commonly used antibiotics, making it challenging to eliminate the infection with chemical methods alone (Hollenbeck and Rice 2012). Therefore, alternative approaches, such as antimicrobial photodynamic therapy (aPDT), have been explored to enhance the efficacy of chemical treatments (Nunes et al. 2022). A significant advantage of aPDT compared to traditional treatment approaches is its capacity to penetrate deeply into the root canal system, reaching areas that are difficult to access with standard instruments (Plotino et al. 2019). Moreover, aPDT has demonstrated a synergistic effect when combined with conventional treatment methods, potentially resulting in improved treatment outcomes and shorter treatment durations (Martins Antunes de Melo et al. 2021). aPDT is a promising approach to combat microbial infections by employing a combination of a photosensitizer, light, and oxygen to generate reactive oxygen species (ROS) that can effectively eliminate bacteria, viruses, and fungi (Pourhajibagher et al. 2016). Traditionally, synthetic photosensitizers have been utilized in aPDT; however, natural photosensitizers have emerged as a potential alternative due to their biocompatibility, low toxicity, and availability (Polat and Kang 2021).

Kojic acid, a natural metabolite derived from fungi, exhibits antimicrobial properties against a various bacteria and fungi (Zilles et al. 2022). While it can be activated by ultraviolet A (UVA) light, its maximum absorption occurs in the UVB range (Pourhajibagher et al. 2023a). Due to the heightened cancer risk associated with UVA light penetration, clinical applications of aPDT using Kojic acid favor visible light sources (400–800 nm), which can penetrate the target site effectively without causing significant damage to surrounding healthy tissues (Gholami et al. 2023; Pourhajibagher et al. 2023b). Similarly, Parietin, a natural pigment found in lichens and plants, shows broad-spectrum antimicrobial activity (Basile et al. 2015; Comini et al. 2017; Mugas et al. 2021a) and enhances the efficacy of aPDT by increasing ROS production (Mugas et al. 2021a; Ayoub et al. 2022a, b). Parietin's absorption spectrum ranges from UVB to visible light, with peak absorption occurring around 430 nm, making light sources within this wavelength range suitable for exciting Parietin in aPDT applications (Fernández-Marín et al. 2018).

The effectiveness of aPDT can be influenced by various factors (Carrera et al. 2016; do Prado-Silva et al. 2022). Therefore, identifying the specific target site(s) within the bacterial cell that is most susceptible to ROS-induced damage can enhance the efficiency of aPDT, potentially leading to the development of more effective and targeted antimicrobial treatments. Previous investigations have revealed that *in silico* analysis—utilizing computational methods and algorithms to explore biological systems—is an integral part of drug discovery, allowing for the identification of target sites for the development of candidate drugs (Ekins et al. 2007; Agamah et al. 2020; Shaker et al. 2021; Pourhajibagher and Bahador 2024). In this study, we began by following a comprehensive workflow to identify the potential of Kojic acid and Parietin against Ace and Esp proteins in *E. faecalis* through various computational methods (Fig. 1). We then investigated the minimum inhibitory concentration (MIC) of Kojic acid and Parietin and subsequently evaluated the changes in the expression of the *esp* and *ace* genes involved in *E. faecalis* biofilm formation following treatment with the aPDT process.

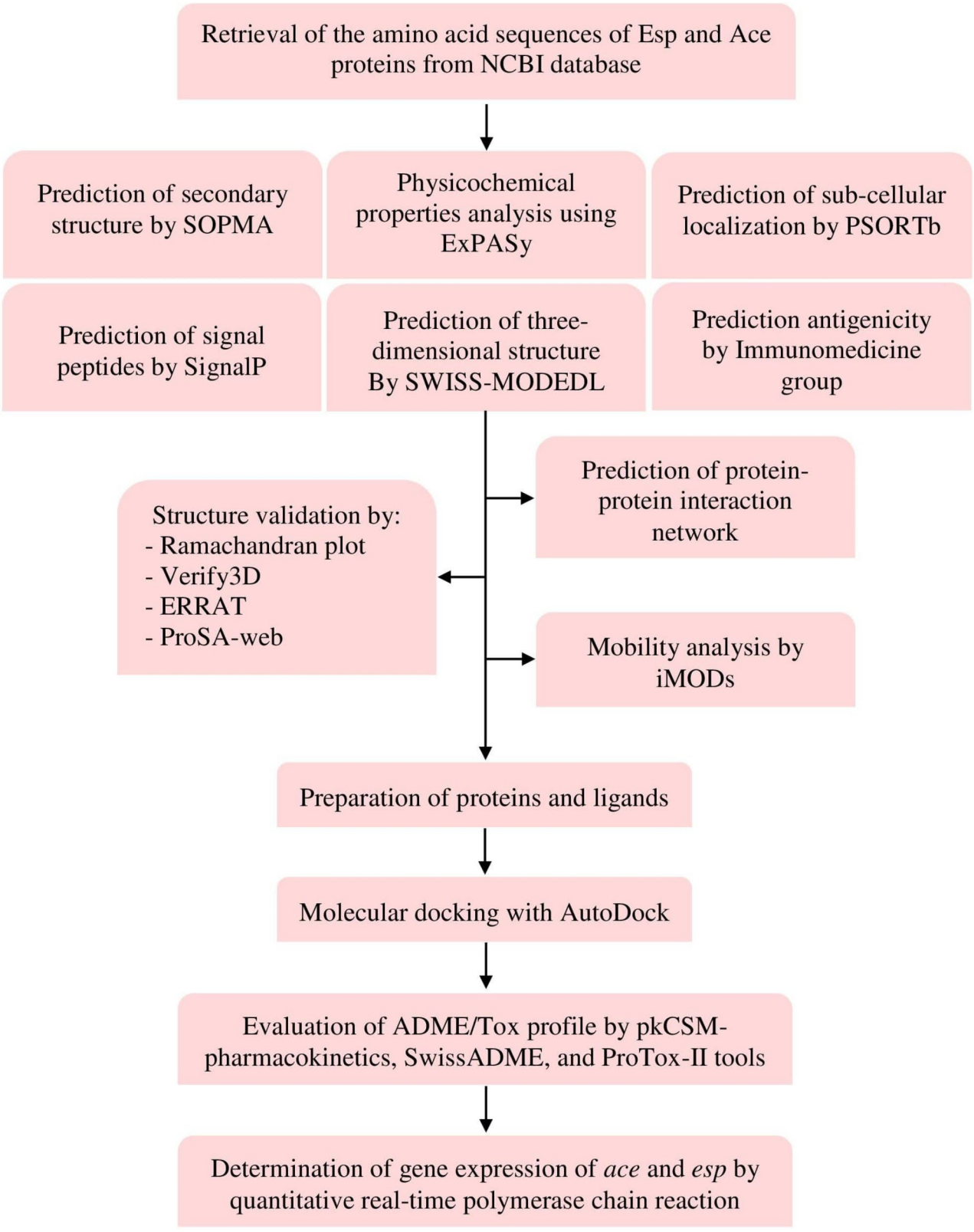

Fig. 1 Flowchart depicting the workflow of virtual screening

Materials and methods

Protein preparation

The National Center for Biotechnology Information (NCBI) database (https://www.ncbi.nlm.nih.gov/) was utilized to retrieve the sequences of the Esp and Ace proteins, identified by accession numbers AEG79633 and WP_271104706, respectively. The amino acid sequences of these proteins were subjected to the Protein-Basic Local Alignment Search Tool (BLASTP) (http://blast.ncbi.nlm.nih.gov/Blast) to find an appropriate template. To predict the secondary structures of Esp and Ace, the Self-Optimized Prediction Method with Alignment (SOPMA) server (https://npsa-prabi.ibcp.fr/cgi-bin/npsa_automat.pl?page=/NPSA/npsa_sopma.html) was employed. Furthermore, the three-dimensional structures of Esp and Ace, with PDB IDs 6ORI and 2Z1P respectively, were achieved from the RCSB Protein Data Bank.

Analysis of physicochemical properties

The physicochemical properties of the selected proteins, including molecular weight, amino acid composition, total number of positive and negative residues, theoretical pI, instability index (II), aliphatic index (AI), extinction coefficient, and grand average of hydropathicity (GRAVY) value were obtained using the ProtParam tool (https://web.expasy.org/protparam/) on the ExPASy server. Additionally, PSORTb v3.0.2 (https://www.psort.org/psortb/), SignalP v6.0 (https://services.healthtech.dtu.dk/services/SignalP-6.0/), and Immunomedicine group (http://imed.med.ucm.es/Tools/antigenic.pl) were used to analyze the sub-cellular localization, signal peptides, and antigenicity of Ace and Esp proteins.

Model quality assessment

The quality of modeled structures was validated by ProSA (https://prosa.services.came.sbg.ac.at), PROCHECK, ERRAT, and Verify3D modules of the SAVES server (https://saves.mbi.ucla.edu/). The SWISS-MODEL Structure Assessment tool (https://swissmodel.expasy.org/assess) and QMEAN tool (https://swissmodel.expasy.org/qmean/) were collaboratively utilized to estimate the QMEAN Z-score and global quality of the models.

Protein-protein interaction (PPI) analysis

A protein network database (https://string-db.org/) was used to determine possible PPIs and present them under a network topology, highlighting the functional characteristics of the Esp and Ace proteins.

Ligands preparation

The structures of the natural compounds (Kojic acid [($C_6H_6O_4$] and Parietin [$C_{16}H_{12}O_5$]) were retrieved from the PubChem Compound Database (http://pubchem.ncbi.nlm.nih.gov).

Molecular docking

Molecular docking approach was employed to investigate the molecular interaction between selected compounds, Kojic acid and Parietin, and the proteins with PDB IDs 2Z1P and 6ORI. The protein-ligand docking simulation was performed using AutoDock4.2 software package. The partial charges of the ligand atoms were calculated using the Gasteiger-Marsili procedure implemented in the AutoDock tools package. Missing hydrogen atoms were added to the proteins, and after determining the Kolman united atom charges, non-polar hydrogens were merged with their corresponding carbons using Autodock tools. For the flexible-ligand docking studies, the Lamarckian Genetic Algorithm (LGA) was utilized to search for the global optimum binding positions, using the default parameters of the AutoDock 4.2 program.

Prior to the docking simulations, the ligands were optimized for conformation using Avogadro software. For the receptors, water molecules, small ligands, and heteroatoms were removed, and their structures were then energy minimized. Finally, 200 independent docking runs were carried out for each ligand-protein complex. The resulting docking poses were analyzed usiung Discovery Studio Visualizer software, which generated two-dimensional and three-dimensional diagrams of the docked protein-ligand structures.

Molecular dynamics simulation

The molecular dynamics simulation study of natural photosensitizers and Esp and Ace docked complex was performed by iMODS (https://imods.iqfr.csic.es/).

Prediction of ADME/Tox profiling by computational analysis

The drug-likeness of Kojic acid and Parietin was assessed using the method established by Lipinski et al. (2004). The *in silico* ADME/Tox profiles of these natural compounds, which include absorption, distribution, metabolism, excretion, and toxicity, was determined using the pkCSM-pharmacokinetics tool (http://structure.bioc.cam.ac.uk/pkcsm) and SwissADME tool (http://www.swissadme.ch/). Moreover, the toxicological characteristics of Kojic acid and Parietin such as LD_{50} values in mg/kg, toxicity class, hepatotoxicity, immunotoxicity, cytotoxicity, mitochondrial toxicity, nephrotoxicity, and mutagenicity were revealed using ProTox-II (https://tox-new.charite.de/protox_II/).

Determination of MIC doses of Kojic acid and Parietin

Stock solutions of both natural compounds were prepared, and their MIC values were determined according

to the Clinical and Laboratory Standards Institute (CLSI) guideline (2015). Serial dilutions were made in Mueller Hinton broth medium (Merck, Germany) on the round-bottom 96-well microplate. The dilution ranges of Kojic acid and Parietin (both purchased from Sigma-Aldrich, Germany: 99% purity) were 0.5–256 mg/mL. After that, 100 µL of *E. faecalis* ATCC 29,212 suspension, adjusted to a final concentration of 1.5×10^6 CFU/mL, was added to each dilution. The microtiter plate was then incubated for 24 h at 37 °C, and the MIC was defined as the lowest concentration of the compound that inhibited visible microbial growth.

RNA extraction and quantitative real-time polymerase chain reaction (qRT-PCR)

Immediately following the treatment of *E. faecalis* with sub-MIC doses of Kojic acid and Parietin, combined with a continuous blue laser (ASHA, Iran) at a wavelength of 450±5 nm and an output intensity of 150 mW/cm^2 for one min, the total RNAs were extracted by the super RNA extraction Kit (AnaCell, Iran). After removing any remaining genomic DNA using RNase-free DNase I treatment, total RNA (150 ng) was reverse transcribed into a 10 µL cDNA reaction volume using the RevertAid First Strand cDNA Synthesis Kit (AnaCell, Iran), following the manufacturer's instructions. Specific primers for the *esp*, *ace*, and *16s rRNA* genes (used as an internal control for standardizing qRT-PCR data) were designed as follows: *ace*-F TCGTCCGTTACACTTCGACA, *ace*-R TCCACATTTTGATTGCCGCT, *esp*-F GGTGATGG AAACCCTGACGA, *esp*-R AGTTGCGCTTTGTGAT CTGT, *16s rRNA*-F GTCGAACGCTTCTTTCCTCC, and *16s rRNA*-R AGCGCCTTTCACTCTTATGC, using Primer3 software; version 4.0 (http://primer3.ut.ee/). qRT-PCR was conducted with a LightCycler® 96 System (Roche Diagnostics, Indianapolis, IN) following cycling parameters: one cycle of denaturation at 95 °C for 5 min, followed by 40 cycles of 15 s at 95 °C, 10 s at 60 °C, and 20 s at 72 °C. Gene expression was quantified relative to controls using the comparative CT method (Schmittgen and Livak 2008).

Statistical analysis

Data analysis was conducted using SPSS version 25.0 (IBM, New York, NY, USA) through one-way analysis of variance (ANOVA). A significance level of $P<0.05$ was established to determine statistical significance in all analyses.

Results

Retrieval of Esp and Ace proteins

A similarity search using BLASTP against target proteins in *E. faecalis* revealed that the Ace and Esp were similar to the protein structures with PDB IDs: 2Z1P and 6ORI, respectively. The alignment between Ace and 2Z1P yielded a total score of 671, with 49% query cover and 95.54% identity. Similarly, the alignment between Esp and 6ORI showed a query cover of 19%, identity of 100%, and a total score of 124.

Prediction of secondary structure

The secondary structure of protein chains was analyzed by SOPMA. For the target protein Ace, the designed secondary structure revealed that random coils comprised 50.15%, followed by alpha helices at 24.63%, extended strands at 20.77%, and beta-turns at 4.45%. The secondary structure composition of Esp protein contained 48.48, 27.27, 15.49, and 8.75% of random coils, extended strands, alpha helices, and beta-turn, respectively. These results indicate that both Ace and Esp proteins predominantly exhibit a coiling structure.

Three-dimension structure and validation

The three-dimensional structures of Ace and Esp proteins were were obtained from the RCSB PDB (Fig. 2). As shown in Fig. 2a, Esp has a resolution of 1.40 Å and consists of one chain and one calcium ion (Ca^{2+}), while Ace has a resolution of 2.50 Å and contains only one chain (Fig. 2b). The interaction of Ca^{+2} with surrounding amino acids is shown in Fig. 2c. Additionally, the modeled ribbon structure and surface view of Ace and Esp proteins are shown in supplementary Figure S1.

The structural quality of the modeled proteins was assessed using a Ramachandran plot, which revealed that 84.1% of the total residues (211) of predicted model evaluation of the Ace protein (PDB 2Z1P) were in favoured regions (A, B, L), while predicted model evaluation of the Esp protein (PDB 6ORI) showed 87% (295) of residues in favoured regions. As seen in the image a of Figs. 3A and B and 12.1% (41) and 15.1% (38) of the residues of 6ORI and 2Z1P, respectively were found in the additional allowed regions (a, b, l, p); 0.6% (2) and 0.3% (1) residues of 6ORI were in the generously allowed (~a, ~b, ~l, ~p) and disallowed regions (XX), respectively, while there were 0% residues of 2Z1P in the disallowed regions and only 0.8% (2) of residues in the generously allowed regions, thus confirming that both predicted models are of high-quality.

ProSA-web predicted the Z-scores of − 5.98 and −6.97 for the Ace and Esp proteins, respectively, suggesting good overall model quality (Images b and c of Fig. 3A and B). Moreover, the structures passed in the validation analysis by Verify3D showed that 89.01 and 99.48% of the residues of predicted model evaluation of the Ace and Esp proteins, respectively have a 3D-1D score ⩾0.1 on average and at least 80% of the amino acids had scored>=0.1 in the 3D/1D profile. ERRAT predicted the quality score of the Ase model as 88.6719, while for the Esp model, the

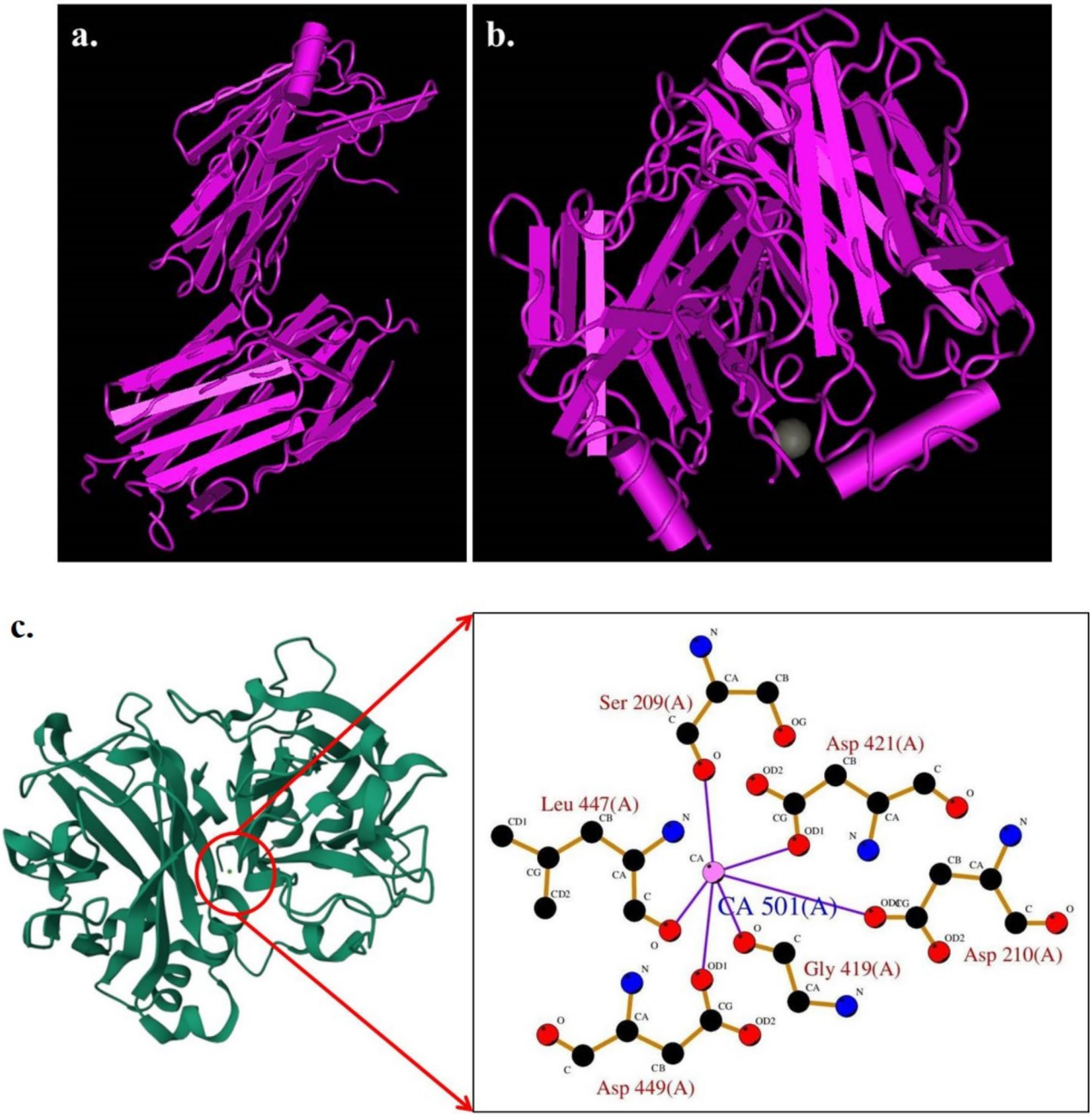

Fig. 2 Three-dimensional structure of proteins: (a) Ace (PDB ID: 2Z1P), (b) Esp (PDB ID: 6ORI), (c) Interaction of Calcium ion (Ca^{+2}) with surrounding amino acid residues of Esp protein

predicted overall quality factor was 94.6381 (Image d of Fig. 3A and B). Additionally, the global scores for Ace and Esp proteins were 0.88±0.05 and 0.94±0.05, respectively, reflecting the reliability of the predicted structures. These findings confirm that the constructed models are of high quality and suitable for predicting active sites and for docking ligands such as Kojic acid and Parietin with Ase and Esp proteins of *E. faecalis*.

Physiochemical profiling of Esp and Ace proteins

The molecular profile analysis revealed 297 and 674 amino acids in Esp and Ace proteins, respectively. A comprehensive examination of these proteins, based on physicochemical characteristics, is detailed in Table 1. According to the data, the grand average of hydropathicity (GRAVY) index was −0.648 for Esp and −0.661 for Ace, indicating that both proteins are hydrophilic, a finding further supported by Kyte and Doolittle hydropathy plot (Figure S2). The predicted antigenic peptide tool

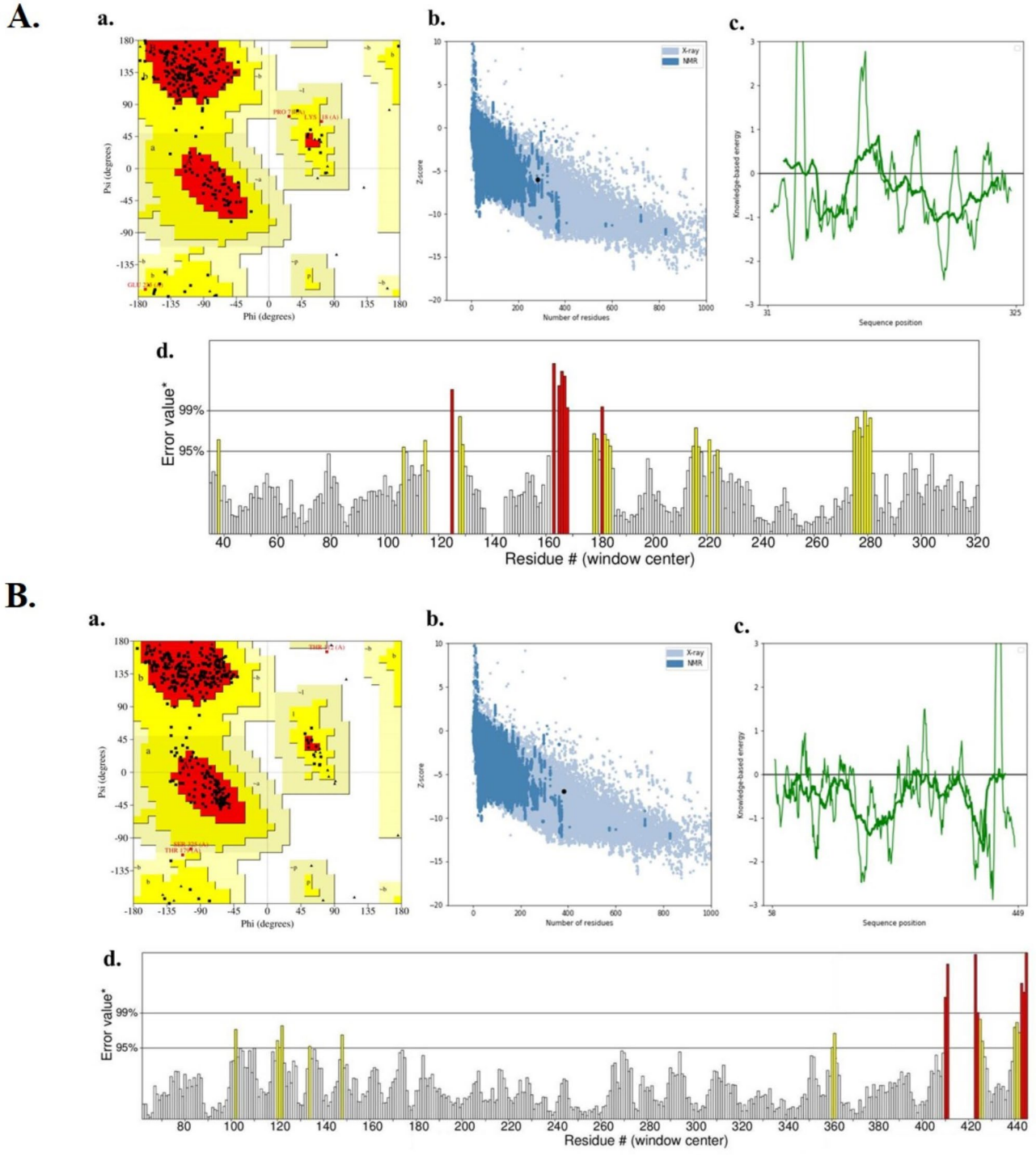

Fig. 3 Validation of predicted structure: (**A**) Ace, (**B**) Esp; (a) Ramachandran plot, (b) Local model quality at ProSA-web, (c) Overall model quality at ProSA-web, and (d) ERRAT

revealed that Esp contains 11 antigenic determinants, while Ace has 25, with average antigenic propensities of 1.0003 and 1.0048, respectively (Figure S3 and Table S1).

Sub-cellular localization of the prokaryotic domain predicted that Ace is associated with the cell wall, whereas Esp is classified as cytoplasmic. Additionally, analysis of proteins by SignalP suggested that 0.0962, 0.008, and 0.006 sequences of Ace signal peptide belonged to the Sec/SPI, Tat/SPI, and Sec/SPII pathways, respectively (Figure S4a). In contrast, Esp's signal peptide sequences were found to be 0.009, 0.009, and 0.001 for the Sec/

Table 1 Molecular and physiochemical properties of Ace and Esp proteins

Molecular and physiochemical profiling	Ace		Esp	
Molecular weight	74184.55		32763.25	
Theoretical pI	4.38		4.37	
Total number of negatively charged residues (Asp + Glu)	117		61	
Total number of positively charged residues (Arg + Lys)	49		33	
Atomic composition	Carbon	3233	Carbon	1456
	Hydrogen	5105	Hydrogen	2265
	Nitrogen	843	Nitrogen	361
	Oxygen	1134	Oxygen	492
	Sulfur	8	Sulfur	2
Formula	$C_{3233}H_{5105}N_{843}O_{1134}S_8$		$C_{1456}H_{2265}N_{361}O_{492}S_2$	
Total number of atoms	10,323		4576	
Extinction coefficients in H_2O (280 nm)	27,390		24,410	
Estimated half-life: The N-terminal of the sequence considered is M (Met)	30 h (mammalian reticulocytes, in vitro). > 20 h (yeast, in vivo). > 10 h (*Escherichia coli*, in vivo)		5.5 h (mammalian reticulocytes, in vitro). 3 min (yeast, in vivo). 2 min (*Escherichia coli*, in vivo)	
Instability index (II)	46.43		26.98	
Aliphatic index	72.26		73.16	
Grand average of hydropathicity (GRAVY)	–0.661		–0.648	

SPI, Tat/SPI, and Sec/SPII pathways, respectively (Figure S4b).

Prediction of PPI

The PPI network analysis conducted using the STRING database showed that our target proteins of interest have interactions with other proteins. Some of these proteins have experimentally known functions, while others remain functionally uncharacterized (Figure S5 and Table S2). In the PPI network for Ace there were 11 nodes, 55 edges, an average node degree of 10, a local clustering coefficient of 1, and a PPI enrichment P-value of 1.24e-14. In contrast, the PPI network for Esp comprised 11 nodes and 32 edges, with an average node degree of 5.82, a local clustering coefficient of 0.888, and a PPI enrichment P-value of 4.29e-06.

Molecular docking

The docking results were analysed and ranked based on their dock score values. Figure 4 illustrates the molecular interactions between Kojic acid and Parietin with the proteins 2Z1P and 6ORI. Table 2 presents the estimated free binding energy values (ΔGbind) of the docked positions, intermolecular energy, electrostatic energy, total internal energy, torsional energy, and inhibition constant (Ki) of these ligands/inhibitors for the respective proteins.

The molecular docking analysis demonstrated that the proteins 2Z1P and 6ORI exhibited the strongest binding affinity for the Parietin ligand, resulting in the lowest inhibition constant (Ki) values of 9.05 and 3.18, respectively. Conversely, Kojic acid displayed weaker interaction compared to Parietin, leading to a higher inhibition constant for this ligand. Notably, the interaction between Kojic acid and 6ORI showcased more favorable binding energy and inhibition constant. Table 2 further corroborates that both Kojic acid and Parietin exhibited superior binding affinity towards the 6ORI protein. The docking analysis highlighted the occurrence of the best bound conformation in the case of 6ORI-Parietin interaction, with a binding energy of–7.83 Kcal/mol and an inhibition constant (Ki) of 3.18 µM. It reinforces the conclusion that both ligands have a greater binding affinity for 6ORI compared to 2Z1P, which is essential for understanding their potential roles in therapeutic applications.

Molecular dynamics simulation

The normal mode analysis (NMA) of Ace and Esp was illustrated in image a of Fig. 5A and B. The main-chain deformability, shown in image b, represents regions in the protein with high deformability. Esp exhibited more significant deformability, with numerous peaks around a deformability index of 1.0, compared to Ace. The B-factor calculated by NMA and shown in image c, suggests the flexibility of proteins based on atomic displacement parameters. Image d represents the eigenvalue of the proteins, which are related to the energy required to deform the structure. Easier deformation occurs when the eigenvalue is lower. Our findings demonstrated that Ace and Esp generated eigenvalues of 1.558461e-04 and 4.887245e-04, respectively. The variance plots illustrated in the image e demonstrate cumulative variances in green colour while individual variances are in violet colour. The covariance matrix between the pairs of residues, shown in image f of Fig. 5A and B, indicates their correlations. Red coloration indicates good correlation between residues, white coloration depicts no correlation, and blue indicates anticorrelations. Moreover, the elastic network model in image g suggests the connection between atom pairs and springs. Each dot in the graph is colored based on the stiffness where the dark grey dots indicate the

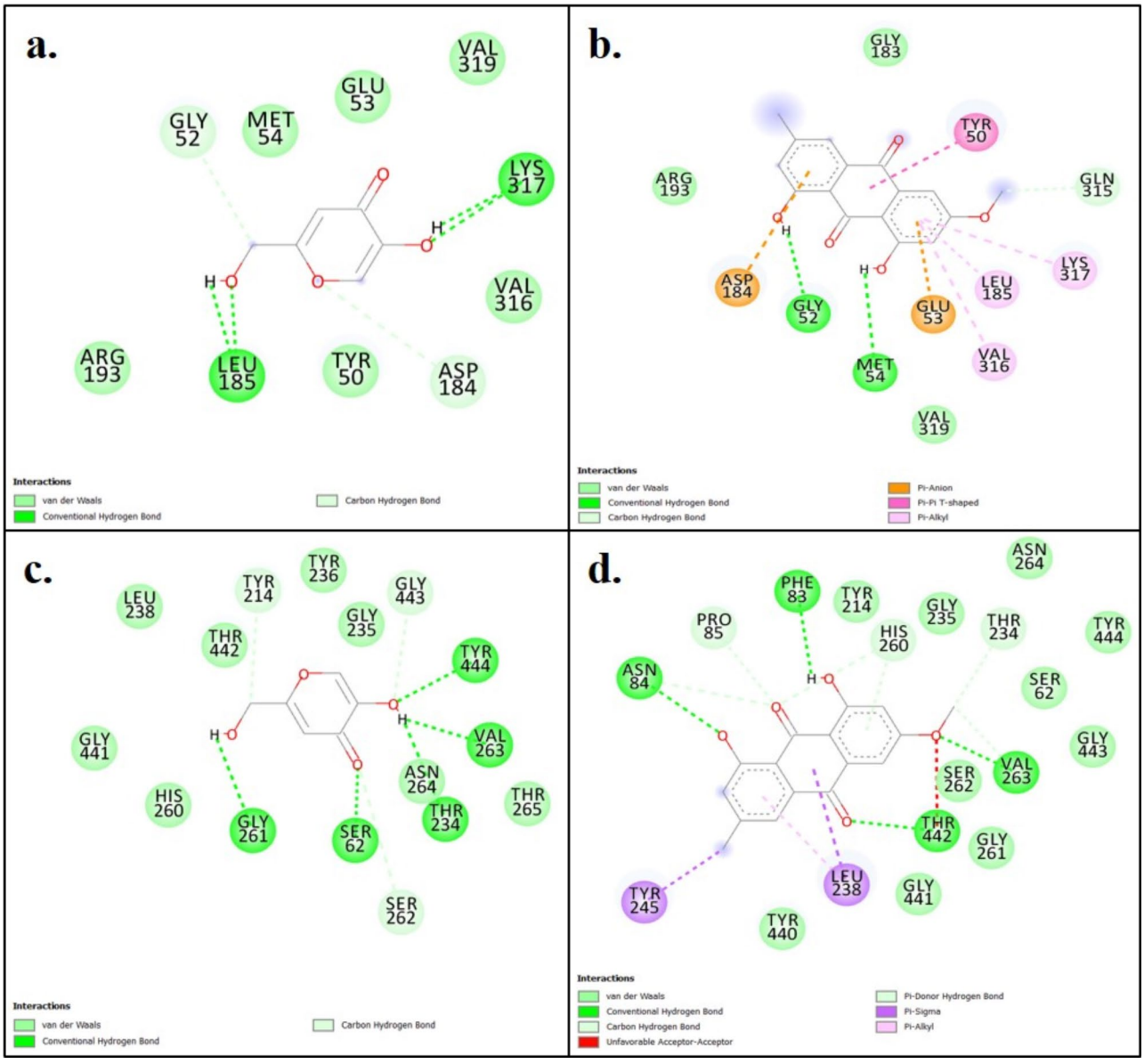

Fig. 4 Two-dimensional diagram of docked protein-ligand complexes. (a) 2Z1P-Kojic acid, (b) 2Z1P-Parietin, (c) 6ORI-Kojic acid, and (d) 6ORI-Parietin

Table 2 Docking results of Kojic acid and parietin docked into 2Z1P and 6ORI proteins

Protein	Ligand	Binding energy	Intermolecular energy	Electrostatic energy	Total internal energy	Torsional energy	Inhibition constant (Ki) (μM)	Active site residues
2Z1P	Kojic acid	−4.76	−5.66	−0.2	−0.78	0.89	323.74	LEU185, LYS317
	Parietin	−6.88	−7.78	−0.13	−1.33	0.89	9.05	GLY52, GLU53, MET54, TYR50, ASP184, LEU185, VAL316, LYS317
6ORI	Kojic acid	−5.97	−6.86	−0.13	−0.78	0.89	42.41	SER62, GLY261, VAL263, ASN264, GLY443, TYR444
	Parietin	−7.83	−8.4	−0.07	−1.34	0.89	3.18	PHE83, ASN84, PRO85, THR234, LEU238, TYR245, HIS260, VAL263, THR442

*The energy values are expressed in kcal/mol

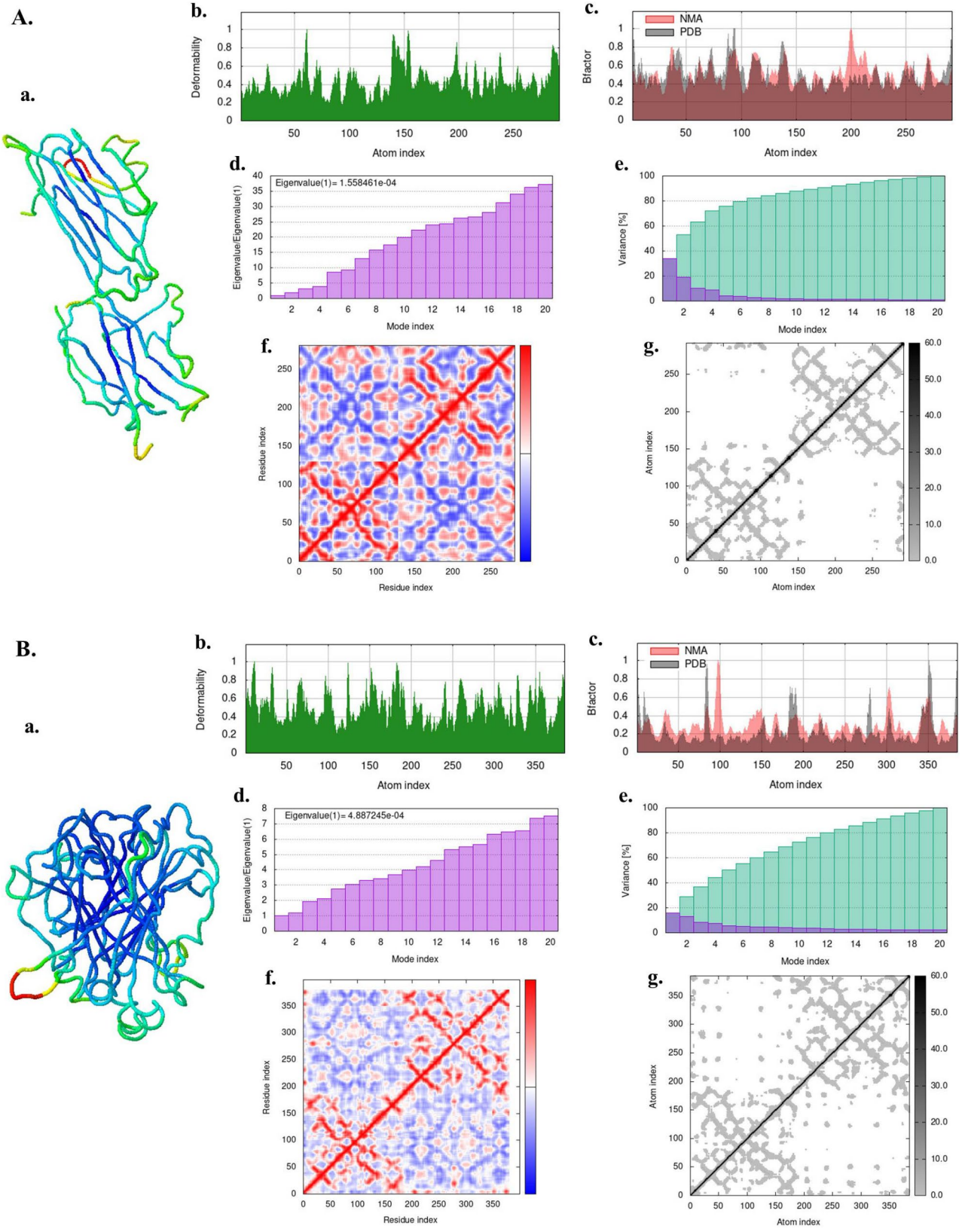

Fig. 5 Molecular dynamic simulation: (**A**) Ace, (**B**) Esp. (a) NMA mobility, (b) Deformability, (c) B-factor values, (d) Eigenvalues, (e) Variance (violet: individual variances, green: cumulative variances), (f) Co-variance map (residues with correlated motions in red, uncorrelated motions in white, and anti-correlated motions in blue), and (g) Elastic network (darker grays indicate stiffer springs) of the complex

Table 3 Drug-likeness characteristics of Kojic acid and parietin

Drug-likeness properties	Kojic acid	Parietin
Formula	C6H6O4	C16H12O5
Molecular weight	142.11 g/mol	284.26 g/mol
Number of H-bond acceptor	4	5
Number of H-bond donor	2	2
Number of rotatable bonds	1	1
LogP	1.12	2.45
TPSA	70.67 $Å^2$	83.83 $Å^2$
Lipinski's rule of five violation	Yes	Yes
Bioavailability score	0.55	0.55

Table 4 Pharmacokinetic properties of Kojic acid and parietin

Standard parameters	Kojic acid	Parietin
Absorption		
Water solubility (LogS)	-0.228	-3.543
HIA (%)	91.39	99.21
GIA	High	High
Caco-2 permeability	0.5133	0.8258
Human oral bioavailability	0.5143	0.5857
Distribution		
BBB	0.5250	0.8000
BPPB (%)	0.327	1.039
P-gp inhibitior	Non-inhibitor	Non-inhibitor
P-gp substrate	Non-substrate	Non-substrate
Metabolism		
CYP3A4 substrate	✗	✗
CYP2C9 substrate	✗	✗
CYP2D6 substrate	✗	✗
CYP3A4 inhibition	✗	✗
CYP2C9 inhibition	✗	✗
CYP2C19 inhibition	✗	✗
CYP2D6 inhibition	✗	✗
CYP1A2 inhibition	✗	✓
Toxicity		
Class	3	5
LD50	550 mg/kg	5000 mg/kg
hERG	Weak inhibitor	Weak inhibitor
Hepatotoxicity	Inactive	Inactive
Carcinogenicity	Active	Inactive
Immunotoxicity	Inactive	Active
Mutagenicity	Active	Active
Respiratory toxicity	Active	Inactive
Cytotoxicity	Inactive	Inactive

Abbreviations: HIA: human intestinal absorption (%); GIA: gastrointestinal absorption; Caco-2: colorectal carcinoma; BBB: blood-brain barrier; BPPB: blood plasma protein binding; P-gp: P-glycoprotein; CYP: cytochrome; hERG: human ether-à-go-go related gene channel inhibition

stiffer springs and lighter grey dots predict flexible ones. The iMOD study of target proteins clearly demonstrates that our proposed proteins are stable.

Evaluation of drug-likeness properties

The drug-likeness properties of Kojic acid and Parietin were assessed by five different filters such as Lipinski, Ghose, Veber, Egan, and Muegge. Both natural compounds adhered to Lipinski's rule of five without any violations (Table 3). At the same time, Kojic acid and Parietin also were found to comply with Veber and Egan rules, showing no violations for these criteria. Other rules were also evaluated to determine the drug-likeness of Kojic acid and Parietin. As the results show, Parietin had no violation of Ghose and Muegge rules, while Kojic acid did not fit with the guidelines of these rules.

Evaluation of ADME/Tox properties

Pharmacokinetic variables can be used to estimate the absorption, distribution, metabolism, elimination (ADME), and toxicity (ADME/Tox) of leading drug candidate molecules. Key ADME/Tox properties evaluated included topological surface area (TPSA), the number of rotatable bonds, water solubility (Log S), human intestinal absorption (HIA), blood-brain barrier (BBB) permeability, access to P-glycoprotein (P-gp) substrates, and cytochrome enzymes (CYP) (Table 4). The ADME/Tox profiling displayed that there were no absorption-related side effects for any of the candidate compounds. According to the boiled-egg chart (Figure S6), Kojic acid and Parietin were identified as non-P-gp substrates, meaning they are not expelled from the cell by the P-gp carrier protein. Additionally, these findings indicated that the natural compounds do not possess BBB permeability.

MIC of natural photosensitizers

After 24 h of incubation, turbidity was noticed in the test wells containing Kojic acid at concentrations ranging from 0.5 to 32 µg/mL, indicating the growth of *E. faecalis*. In contrast, no turbidity was detected at concentrations of 64, 128, and 256 µg/mL, demonstrating inhibition of bacterial growth. Considerable turbidity was also observed in the wells containing Parietin at the concentrations of 0.5, 1, 2, 4, and 8 µg/mL, while there was no turbidity at concentrations above 16 µg/mL. Therefore, the MICs were determined to be 16 µg/mL for Parietin and 64 µg/mL for Kojic acid against *E. faecalis*.

Effect of natural photosensitizers-mediated aPDT on gene expression

In this study, qRT-PCR was employed to evaluate the expression levels of the *ace* and *esp* genes in *E. faecalis* following treatment with sub-MIC concentrations of Kojic acid and Parietin, combined with laser light exposure. The qRT-PCR results presented in Fig. 6 indicate that the expression of the ace gene significantly decreased by 3.75-fold and 5.32-fold, respectively, when treated with sub-MIC concentrations of Kojic acid (32 µg/mL) and Parietin (8 µg/mL) combined with one min of laser light exposure, compared to the control group (untreated *E. faecalis*; $P<0.05$). Similarly, the expression of the *esp*

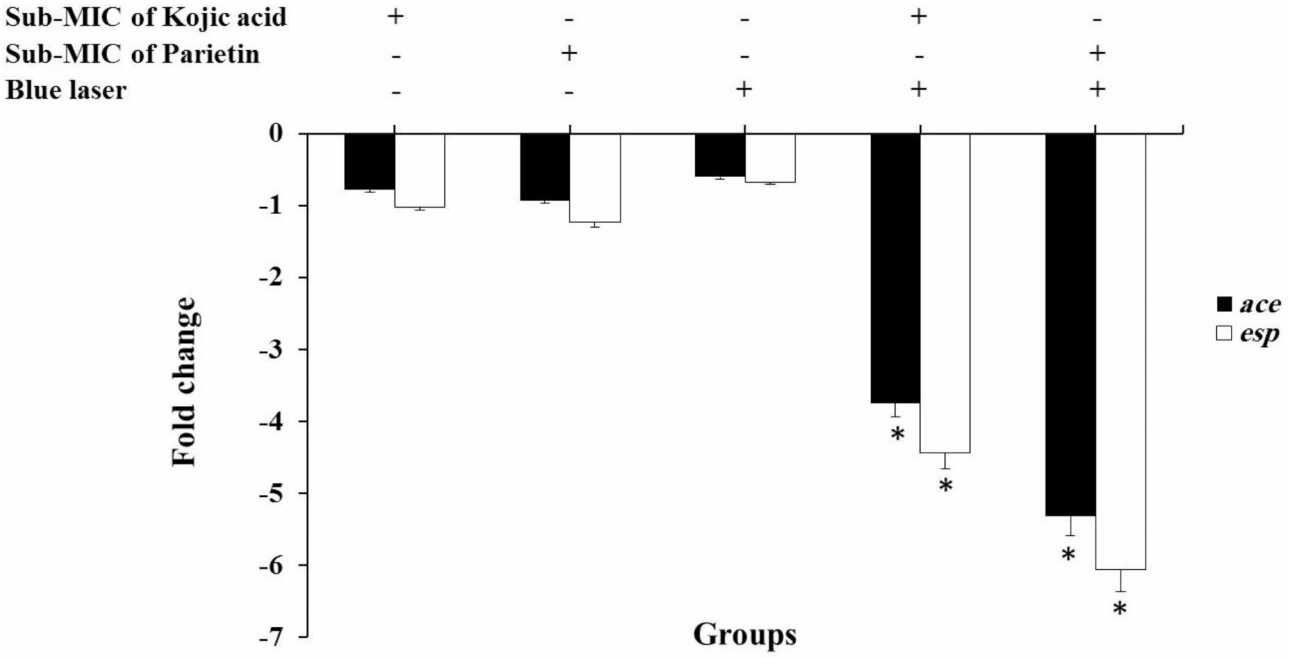

Fig. 6 Effect of natural photosensitizers-mediated aPDT on gene expression of *ace* and *esp*. *Significantly different from the control group (no treatment), $P < 0.05$

gene was downregulated by 4.44-fold and 6.06-fold, respectively, following treatment with aPDT using sub-MIC concentrations of Kojic acid and Parietin, relative to the control group (Fig. 6). As shown in Fig. 6, the sub-MIC treatment groups did not show any significant effect on the expression of *ace* and *esp* genes ($P > 0.05$). Additionally, the levels of *ace* and *esp* were downregulated by 0.61- and 0.68-folds, respectively after exposure to laser light onle, with no significant difference compared to the control group ($P > 0.05$).

Discussion

Studies have shown that *E. faecalis* can lead to persistent infections and reinfections in root canals, often resulting in treatment failures (Zoletti et al. 2006; Ali et al. 2020; Voit et al. 2022; Carlesi et al. 2023). Biofilm formation is a significant virulence factor for *E. faecalis*, enabling the bacterium to colonize various surfaces and resist antimicrobial treatments (Alghamdi and Shakir 2020). The *esp* and *ace* genes play important roles in the initial attachment and aggregation of *E. faecalis* cells, which are critical steps in biofilm formation (Francisco et al. 2001; Francisco et al. 2021).

Recently, targeted aPDT has emerged as a promising adjuvant treatment for combating microbial biofilms (Ribeiro et al. 2022). For effective targeted aPDT, selecting an appropriate photosensitizer is crucial. A clinically effective photosensitizer should possess a certain degree of hydrophilicity to prevent accumulation and should specifically bind to target regions on microbial cells. This specificity enhances internalization at the target site and minimizes unwanted off-target effects (Ghorbani et al. 2018).

In this *in silico* study, Kojic acid and Parietin are proposed as natural photosensitizers that interact with Ace and Esp proteins, which are essential for the formation and development of *E. faecalis* biofilms. *In silico* analysis, utilizing computational methods and algorithms to investigate biological systems, can be instrumental in identifying target sites on microbial proteins.

Predicting the secondary and three-dimensional structures of the target proteins is crucial for future analysis. In this study, random coils were identified as the optimum scaffolded structure in the designed secondary structures of Ace (50.15%) and Esp (48.48%) proteins. The modeled three-dimensional tertiary structure of the target proteins showed high quality, as assessed by various methods including Ramachandran Plot analysis, Verify3D, ERRAT, and ProSA-web servers. Furthermore, molecular dynamics simulations were conducted to verify the stability of the Ace and Esp structures, and the results indicated that the modeled structures of both proteins were stable, making them reliable targets for Kojic acid and Parietin.

The signal peptide pathway in bacteria is an essential process for transport of proteins across the cell membrane, allowing for their proper function and survival (Schneewind and Missiakas 2014). In Gram-positive bacteria like *E. faecalis*, there are two primary pathways for protein transport across the cell membrane: the secretion

(Sec) pathway and twin-arginine translocation (Tat) pathway (van Wely et al. 2001; Tseng et al. 2009). Both pathways are responsible for the transport of proteins that contain a signal peptide, a short amino acid sequence that directs the protein to the appropriate pathway. The Sec pathway is the most commonly used pathway for protein transport in bacteria, responsible for the translocation of unfolded proteins across the membrane. This pathway involves the SecA ATPase, which binds to the protein's signal peptide and facilitates its transfer across the cytoplasmic membrane. The translocation process requires the presence of a protein channel known as the SecYEG complex, which forms a pore in the membrane. The SecYEG complex is composed of three subunits: SecY, SecE, and SecG, which work in concert to translocate the protein through the membrane (Beckwith 2013; Tsirigotaki et al. 2017).

In contrast, the Tat pathway is responsible for transporting folded proteins that are too large to be moved by the Sec pathway. This pathway involves the proteins TatA, TatB, and TatC, which form a protein channel that allows the transport of folded proteins across the membrane (Goosens et al. 2014; Frain et al. 2019). The Tat pathway is energized by the proton motive force across the membrane (Goosens et al. 2014). In *E. faecalis*, the signal peptide pathways for both Sec and Tat are similar to those in other bacteria. The signal peptide is recognized by the appropriate pathway, directing the protein to either the Sec or Tat system. Once the protein is translocated across the membrane, it can either be folded and functional or undergo further modified by other cellular machinery. In this study, SignalP was used to analyze the protein sequences and predict the pathway used for their transport across the cell membrane. The results indicated that a greater proportion of Ace signal peptides are associated with the Sec/SPI pathway compared to the Tat/SPI and Sec/SPII pathways. In contrast, Esp signal peptides were found across all three pathways, but at a lower frequency. These findings provide insight into the sub-cellular localization and transport mechanisms of Ace and Esp within the bacterial cell, revealing that Ace is located in the cell wall while Esp is found in the cytoplasm.

In this study, the structure-based method using AutoDock4.2 software package was used to predict the active sites of Ace and Esp proteins. The active site of a protein is a critical region where chemical reactions occur. It is typically a small, specific region of the protein that interacts with other molecules, such as substrates, cofactors, or inhibitors (Brooks et al. 1985; Bray et al. 2009; Barnsley and Ondrechen 2022; Weinstein et al. 2023). Predicting the location and properties of the active site is important for understanding the function of a protein, designing inhibitors or drugs, and predicting the effect of mutations or variations on protein function (Sankararaman et al. 2010). Active site prediction involves identifying and characterizing the key residues that contribute to the active site, as well as the shape and electrostatic properties of the site (Barnsley and Ondrechen 2022).

In the current study, the PPI network of Ace and Esp proteins was assessed. PPIs provide a way to visualize and study the complex interactions between proteins, allowing researchers to gain insights into the functional properties of individual proteins as well as the overall function of the network (Rao et al. 2014; Sevimoglu and Arga 2014). Furthermore, PPIs can be used to identify potential drug targets for various diseases. By targeting proteins that are critical nodes in disease-associated PPIs, researchers can potentially disrupt the function of the network and treat the disease (Feng et al. 2017). In this study, we identified critical nodes that play important roles in maintaining the overall stability and function of the network. There was a sum of 22 nodes in the PPI network of Ace and Esp. These nodes are often proteins with a high degree of connectivity, meaning they interact with many other proteins in the network. Disrupting these node proteins due to the aPDT can have a significant impact on the overall function of the network.

Moreover, we evaluated the molecular dynamics simulation of the Ace and Esp proteins. The importance of the prediction of molecular dynamics simulation in proteins is to provide insights into the structural and functional properties of proteins (Sinha et al. 2022). *In silico* studies that determine a protein's deformability enable researchers to explore how conformational changes in the protein can affect its function (Haspel et al. 2010). Many drugs, including photosensitizers, operate by binding to specific protein targets and changing their conformation, either by stabilizing or destabilizing their structures. As the results of the current study showed, the Esp protein exhibited the highest deformability, characterized by numerous peaks. Furthermore, Esp displayed the highest number of eigenvalues, which can be used to predict the protein's normal modes of motion (4.887245e-04). In contrast, the flexibility of various regions of the Ace protein, as determined by its B-factor (also known as the temperature factor), was more than the Esp protein. Other factors evaluated were the variance plot, the elastic network model, and the covariance matrix. The variance plot describes the distribution of fluctuations in the protein's structure and serves as a measure of the protein's flexibility (López-Blanco et al. 2011; López-Blanco et al. 2014). The elastic network model is a computational method that allows for the investigation of the collective motions and dynamics of a protein, which are critical for its function (Fuglebakk et al. 2013). The covariance matrix of a protein also provides valuable insights into the protein's functional dynamics (López-Blanco et

al. 2011). Proteins are dynamic molecules that undergo conformational changes in order to perform their biological functions, and the covariance matrix can help identify regions of the protein that are involved in these dynamic processes (Fuglebakk et al. 2013). According to the results of this study, the most cumulative variances and a good correlation between residues with the flexible springs were observed in Ace protein. Overall, the findings showed that both proposed proteins have stable structures and functional features.

There is currently a lack of information regarding the implications of molecular dynamics simulations on the stability and functional dynamics of proteins during aPDT. However, further research using molecular dynamics simulations has the potential to enhance our understanding of protein stability during aPDT by providing detailed insights into the dynamic behavior of proteins under conditions that mimic physiological and therapeutic environments. Based on literature (Pikkemaat et al. 2002; Salsbury 2010; Sinha et al. 2022), it is expected that molecular dynamics simulations can allow researchers to observe the time-dependent movements of proteins, revealing how structural fluctuations can affect stability. This is crucial during aPDT, as proteins may encounter ROS that can induce conformational changes. By analyzing the trajectories from molecular dynamics simulations, researchers can identify flexible regions within proteins that may be more susceptible to destabilization or denaturation during aPDT. On the other hand, molecular dynamics simulations can assess how proteins respond to thermal stress and photosensitizers used in aPDT. By simulating conditions that mimic these stresses, researchers can evaluate the resilience of proteins like Ace and Esp, determining their likelihood of maintaining functional integrity during treatment. Molecular dynamics simulations can provide insights into how proteins interact with photosensitizers and other therapeutic agents. Understanding these interactions at an atomic level helps in predicting how aPDT will affect protein function and stability, as the binding of ligands can alter the conformational landscape of proteins. The role of water molecules in stabilizing protein structures is highlighted in molecular dynamics studies. Water can mediate interactions between amino acids and influence the overall stability of protein complexes. This is particularly relevant in aPDT, where the generation of reactive species can alter the hydration shell around proteins, potentially impacting their stability and function.

Furthermore, we conducted molecular docking and ADME/Tox analysis to assess the mechanism of action of Kojic acid and Parietin as potential inhibitors of *E. faecalis* biofilm formation during the aPDT process. Molecular docking is used to study and predict the intermolecular interactions between a small molecule (ligand) and a macromolecule (receptor) (Meng et al. 2011). According to the findings, Parietin has significantly lower binding energies (-6.88 and −7.83 Kcal/mol) compared to Kojic acid (-4.76 and −5.97 Kcal/mol) for both Ace and Esp proteins. Lower binding energies indicate stronger binding affinity between the ligand and the protein. Parietin interacts with more active site residues (7 for Ace and 9 for Esp) compared to Kojic acid (2 for Ace and 6 for Esp). A greater number of interactions with active site residues can contribute to the stronger binding affinity of Parietin. The inhibitory constants (Ki) for Parietin are much lower than those for Kojic acid, indicating that Parietin is a more potent inhibitor of both Ace and Esp proteins. Lower Ki values suggest stronger inhibition at lower concentrations. The differences in binding energies and inhibitory constants between the two compounds can be attributed to their structural differences. Parietin, being a larger and more complex molecule, may form more favorable interactions with the proteins, leading to stronger binding and inhibition compared to the smaller and simpler Kojic acid molecule. The lower binding energies, higher number of active site interactions, and lower inhibitory constants suggest that Parietin has a stronger binding affinity and inhibitory potency towards Ace and Esp proteins compared to Kojic acid, based on the provided docking simulation data.

The ADME/Tox profiling of photosensitizers is determined to evaluate their pharmacokinetic properties. ADME/Tox analysis revealed that both natural compounds were soluble in water. The percentages of Kojic acid and Parietin that would be absorbed through the human intestine (HIA%) were predicted to be 91.39 and 99.21%, respectively. Both compounds lack blood-brain barrier (BBB) permeability and exhibit high gastrointestinal absorption without binding to blood plasma proteins. These compounds, with human oral bioavailability, were also predicted to be non-inhibitor and non-substrate of P-gp. Except for CYP1A2, which was inhibited by Parietin, all CYP3A4, CYP2C9, CYP2D6, CYP2C19, and CYP1A2 were predicted to not be inhibited and metabolized by Kojic acid and Parietin. The toxicity data showed a toxicity class of 3 and 5 with LD50 values of 550 and 5000 mg/kg for Kojic acid and Parietin, respectively. Kojic acid was found to be non-hepatotoxic, non-immunotoxic, and non-cytotoxic, while Parietin is non-hepatotoxic, non-carcinogenic, non-toxic to the respiratory system, and non-cytotoxic.

The ADME/Tox analysis revealed that both Kojic acid and Parietin have a molecular mass of less than 500 Da (142.11 and 284.26 g/mol, respectively), adhering to the Lipinski rule. The molecular weight of a drug is important as it affects the absorption rate and amount in the body. Furthermore, both photosensitizers have a suitable hydrogen bond donor count of 2 and a hydrogen bond

receptor count of less than 10, indicating strong binding strength. They also exhibit high lipophilicity, defined as the partition coefficient (logP), which is less than 3, indicating good absorption. In drug development, lipophilicity and molecular weight are often increased to improve the affinity and selectivity of the therapeutic candidate. The molar refractivity of both photosensitizers falls within the acceptable range of 40 to 130 (33.13 for Kojic acid and 75.25 for Parietin).

While *in silico* studies can provide valuable insights into the behavior of biological systems, the results may not always be accurate or reliable since they are based on theoretical models and assumptions. Therefore, it is essential to verify the predictions of *in silico* studies via in vitro study followed by in vivo examination to confirm their validity and relevance to the actual biological systems. When the results of *in silico* studies are examined in vitro, they can be compared to actual experimental data, and any discrepancies or limitations can be identified and addressed. This helps to refine the computational models and algorithms used *in silico* studies, improving their accuracy and reliability. Therefore, in this study, we obtained the MICs of two natural photosensitizers against *E. faecalis* and evaluated their effects along with blue laser irradiation during targeted aPDT on the expression of genes involved in *E. faecalis* biofilm formation in vitro. As the results showed, the MICs of Parietin and Kojic acid against *E. faecalis* were 16 µg/mL and 64 µg/mL, respectively. Traditional antibiotics commonly used to treat *E. faecalis* infections include penicillin (MICs 8–16 µg/mL), ampicillin (MICs 8–16 µg/mL), amoxicillin (MICs 8–16 µg/mL), Ampicillin/sulbactam (MICs≤32/16 µg/mL), vancomycin (MICs 4–32 µg/mL), and tigecycline (MIC≤0.5 µg/mL). The emergence of resistant strains, such as vancomycin-resistant enterococci (VRE), has led to the need for alternative therapies like combination regimens or newer antibiotics including linezolid (MICs 2–8 µg/mL) (CLSI guideline 2019). It is evident that the MICs of Parietin and Kojic acid against *E. faecalis* are higher than those of most traditional antibiotics used for this pathogen. However, it is important to highlight that in aPDT, the activation of photosensitizers by light of a specific wavelength generates ROS. This process significantly enhances the efficacy of the photosensitizers, resulting in a reduction of their MICs against microorganisms during aPDT.

In addition, the expression of *ace* and *esp* genes in *E. faecalis* was significantly downregulated following treatment with aPDT using sub-MIC concentrations of Kojic acid and Parietin, combined with one min of blue laser irradiation, compared to the control group. The qRT-PCR results provide compelling evidence that both Kojic acid and Parietin, particularly when combined with laser light, significantly reduce the expression of the *ace* and *esp* genes in *E. faecalis*. This downregulation can have implications for understanding the potential therapeutic applications of these compounds, especially in contexts where inhibition of these genes is desirable.

The use of natural photosensitizers, such as Kojic acid and Parietin, during targeted aPDT offers several benefits. They are biocompatible, have improved targeting capabilities, are less toxic, reduce resistance, and are often readily available and cost-effective compared to synthetic photosensitizers, making them an attractive option for clinical use. Nevertheless, further research is necessary to explore their full potential as natural photosensitizers in aPDT.

This study found that Kojic acid and Parietin, with drug-likeness properties, could effectively interact with Ace and Esp proteins with strong binding affinities. Targeted aPDT using these compounds could inhibit the biofilm growth of *E. faecalis* by significant downregulation of the expression of *ace* and *esp* genes. As a result, natural photosensitizers-mediated aPDT can be considered a promising adjunctive treatment against endodontic infections. It is necessary to validate the potential antimicrobial activities of these natural compounds through further in vitro and in vivo studies to confirm their effectiveness and ensure their safety profiles for their use in the clinical setting. It is also suggested that the molecular dynamics simulations on the stability and functional dynamics of Ace and Esp proteins during aPDT assessed.

Supplementary Information

The online version contains supplementary material available at https://doi.org/10.1186/s13568-024-01751-y.

Supplementary Material 1

Supplementary Material 2

Acknowledgements
Not applicable.

Author contributions
MP and AB contributed to the study design. MP and ZJ performed the in silico and in vitro examinations. MP wrote the first draft of the manuscript. MP and AB collaborated in analyzing the results. MP, ZJ, and AB edited and approved the manuscript.

Funding
This research was supported by Dental Research Center, Dentistry Research Institute, Tehran University of Medical Science & Health Services grant No. 1401-3-234-62741.

Data availability
All data of this study are included in the manuscript. All figures are original images and have been used for the first time in this study.

Declarations

Conflict of interest
The authors declare no conflict of interest.

Ethical approval

All methods were carried out in accordance with relevant guidelines and regulations. All experimental protocols were approved by the Ethics Committee of Tehran University of Medical Sciences (IR.TUMS.DENTISTRY.REC.1401.123).

Received: 19 March 2024 / Accepted: 14 August 2024
Published online: 31 August 2024

References

Agamah FE, Mazandu GK, Hassan R, Bope CD, Thomford NE, Ghansah A, Chimusa ER (2020) Computational/in silico methods in drug target and lead prediction. Brief Bioinform 21(5):1663–1675. https://doi.org/10.1093/bib/bbz103

Alghamdi F, Shakir M (2020) The influence of *Enterococcus faecalis* as a Dental Root Canal Pathogen on Endodontic Treatment: a systematic review. Cureus 12(3):e7257. https://doi.org/10.7759/cureus.7257

Ali IAA, Cheung BPK, Matinlinna J, Lévesque CM, Neelakantan P (2020) Trans-Cinnamaldehyde potently kills *Enterococcus faecalis* biofilm cells and prevents biofilm recovery. Microb Pathog 149:104482. https://doi.org/10.1016/j.micpath.2020.104482

Ayoub AM, Amin MU, Ambreen G, Dayyih AA, Abdelsalam AM, Somaida A, Engelhardt K, Wojcik M, Schäfer J, Bakowsky U (2022a) Photodynamic and anti-angiogenic activities of parietin liposomes in triple negative breast cancer. Biomater Adv 134:112543. https://doi.org/10.1016/j.msec.2021.112543

Ayoub AM, Gutberlet B, Preis E, Abdelsalam AM, Abu Dayyih A, Abdelkader A, Balash A, Schäfer J, Bakowsky U (2022b) Parietin cyclodextrin-inclusion complex as an effective formulation for bacterial photoinactivation. Pharmaceutics 14(2):357. https://doi.org/10.3390/pharmaceutics14020357

Barnsley KK, Ondrechen MJ (2022) Enzyme active sites: identification and prediction of function using computational chemistry. Curr Opin Struct Biol 74:102384. https://doi.org/10.1016/j.sbi.2022.102384

Basile A, Rigano D, Loppi S, Di Santi A, Nebbioso A, Sorbo S, Conte B, Paoli L, De Ruberto F, Molinari AM, Altucci L, Bontempo P (2015) Antiproliferative, antibacterial and antifungal activity of the lichen Xanthoria parietina and its secondary metabolite parietin. Int J Mol Sci 16(4):7861–7875. https://doi.org/10.3390/ijms16047861

Beckwith J (2013) The Sec-dependent pathway. Res Microbiol 164(6):497–504. https://doi.org/10.1016/j.resmic.2013.03.007

Bray T, Chan P, Bougouffa S, Greaves R, Doig AJ, Warwicker J (2009) SitesIdentify: a protein functional site prediction tool. BMC Bioinformatics 10:379. https://doi.org/10.1186/1471-2105-10-379

Brooks CL 3rd, Brünger A, Karplus M (1985) Active site dynamics in protein molecules: a stochastic boundary molecular-dynamics approach. Biopolymers 24(5):843–865. https://doi.org/10.1002/bip.360240509

Carlesi T, Dotta TC, Pierfelice TV, D'Amico E, Lepore S, Tripodi D, Piattelli A, D'Ercole S, Petrini M (2023) Efficacy of 5% aminolaevulinic acid and red light on *Enterococcus faecalis* in infected Root canals. Gels 9(2):125. https://doi.org/10.3390/gels9020125

Carrera ET, Dias HB, Corbi SCT, Marcantonio RAC, Bernardi ACA, Bagnato VS, Hamblin MR, Rastelli ANS (2016) The application of antimicrobial photodynamic therapy (aPDT) in dentistry: a critical review. Laser Phys 26(12):123001. https://doi.org/10.1088/1054-660X/26/12/123001

Clinical and Laboratory Standards Institute (2019) Performance standards for antimicrobial susceptibility testing; twenty-second informational supplement. CLSI document M100-S22. Clinical and Laboratory Standards Institute, Wayne, PA

Comini LR, Morán Vieyra FE, Mignone RA, Páez PL, Laura Mugas M, Konigheim BS, Cabrera JL, Núñez Montoya SC, Borsarelli CD (2017) Parietin: an efficient photo-screening pigment in vivo with good photosensitizing and photodynamic antibacterial effects in vitro. Photochem Photobiol Sci 16(2):201–210. https://doi.org/10.1039/c6pp00334f

do Prado-Silva L, Brancini GT, Braga GÚ, Liao X, Ding T, Sant'Ana AS (2022) Antimicrobial photodynamic treatment (aPDT) as an innovative technology to control spoilage and pathogenic microorganisms in agri-food products: an updated review. Food Control 132:108527. https://doi.org/10.1016/j.foodcont.2021.108527

Ekins S, Mestres J, Testa B (2007) In silico pharmacology for drug discovery: applications to targets and beyond. Br J Pharmacol 152(1):21–37. https://doi.org/10.1038/sj.bjp.0707306

Feng Y, Wang Q, Wang T (2017) Drug target protein-protein Interaction networks: a systematic perspective. Biomed Res Int 2017:1289259. https://doi.org/10.1155/2017/1289259

Fernández-Marín B, Artetxe U, Becerril JM, Martínez-Abaigar J, Núñez-Olivera E, García-Plazaola JI (2018) Can Parietin Transfer Energy Radiatively to Photosynthetic pigments? Molecules 23(7):1741. https://doi.org/10.3390/molecules23071741

Frain KM, Robinson C, van Dijl JM (2019) Transport of folded proteins by the Tat System. Protein J 38(4):377–388. https://doi.org/10.1007/s10930-019-09859-y

Francisco PA, Fagundes PIDG, Lemes-Junior JC, Lima AR, Passini MRZ, Gomes BPFA (2021) Pathogenic potential of *Enterococcus faecalis* strains isolated from root canals after unsuccessful endodontic treatment. Clin Oral Investig 25(9):5171–5179. https://doi.org/10.1007/s00784-021-03823-w

Fuglebakk E, Reuter N, Hinsen K (2013) Evaluation of protein Elastic Network models based on an analysis of collective motions. J Chem Theory Comput 9(12):5618–5628. https://doi.org/10.1021/ct400399x

Gholami L, Shahabi S, Jazaeri M, Hadilou M, Fekrazad R (2023) Clinical applications of antimicrobial photodynamic therapy in dentistry. Front Microbiol 13:1020995. https://doi.org/10.3389/fmicb.2022.1020995

Ghorbani J, Rahban D, Aghamiri S, Teymouri A, Bahador A (2018) Photosensitizers in antibacterial photodynamic therapy: an overview. Laser Ther 27(4):293–302. https://doi.org/10.5978/islsm.27_18-RA-01

Goosens VJ, Monteferrante CG, van Dijl JM (2014) The Tat system of Gram-positive bacteria. Biochim Biophys Acta 1843(8):1698–1706. https://doi.org/10.1016/j.bbamcr.2013.10.008

Haspel N, Moll M, Baker ML, Chiu W, Kavraki LE (2010) Tracing conformational changes in proteins. BMC Struct Biol 10 Suppl 1(Suppl 1):S1. https://doi.org/10.1186/1472-6807-10-S1-S1

Hollenbeck BL, Rice LB (2012) Intrinsic and acquired resistance mechanisms in enterococcus. Virulence 3(5):421–433. https://doi.org/10.4161/viru.21282

Lipinski CA (2004) Lead- and drug-like compounds: the rule-of-five revolution. Drug Discov Today Technol 1(4):337–341. https://doi.org/10.1016/j.ddtec.2004.11.007

Lopéz-Blanco JR, Garzón JI, Chacón P (2011) iMod: multipurpose normal mode analysis in internal coordinates. Bioinformatics 27(20):2843–2850. https://doi.org/10.1093/bioinformatics/btr497

López-Blanco JR, Aliaga JI, Quintana-Ortí ES, Chacón P (2014) iMODS: internal coordinates normal mode analysis server. Nucleic Acids Res. https://doi.org/10.1093/nar/gku339. W271-6

Martins Antunes de Melo WD, Celiešiūtė-Germanienė R, Šimonis P, Stirkė A (2021) Antimicrobial photodynamic therapy (aPDT) for biofilm treatments. Possible synergy between aPDT and pulsed electric fields. Virulence 12(1):2247–2272. https://doi.org/10.1080/21505594.2021.1960105

Meng XY, Zhang HX, Mezei M, Cui M (2011) Molecular docking: a powerful approach for structure-based drug discovery. Curr Comput Aided Drug Des 7(2):146–157. https://doi.org/10.2174/157340911795677602

Mugas ML, Calvo G, Marioni J, Céspedes M, Martinez F, Vanzulli S, Sáenz D, Di Venosa G, Nuñez Montoya S, Casas A (2021a) Photosensitization of a subcutaneous tumour by the natural anthraquinone parietin and blue light. Sci Rep 11(1):23820. https://doi.org/10.1038/s41598-021-03339-z

Mugas ML, Calvo G, Marioni J, Céspedes M, Martinez F, Sáenz D, Di Venosa G, Cabrera JL, Montoya SN, Casas A (2021b) Photodynamic therapy of tumour cells mediated by the natural anthraquinone parietin and blue light. J Photochem Photobiol B 214:112089. https://doi.org/10.1016/j.jphotobiol.2020.112089

Nunes LP, Nunes GP, Ferrisse TM, Strazzi-Sahyon HB, Cintra LTÂ, Dos Santos PH, Sivieri-Araujo G (2022) Antimicrobial photodynamic therapy in endodontic reintervention: a systematic review and meta-analysis. Photodiagnosis Photodyn Ther 39:103014. https://doi.org/10.1016/j.pdpdt.2022.103014

Pereira TC, Dijkstra RJB, Petridis X, Sharma PK, van de Meer WJ, van der Sluis LWM, de Andrade FB (2021) Chemical and mechanical influence of root canal irrigation on biofilm removal from lateral morphological features of simulated root canals, dentine discs and dentinal tubules. Int Endod J 54(1):112–129. https://doi.org/10.1111/iej.13399

Piantavini MS, Gonçalves AG, Trindade ÂC, Noseda MD, Mercê AL, Machado AE, Pontarolo R (2017) Elucidation of the electronic spectrum changes of KA-Al3 + complex by potentiometric titration, FTIR, 13 C RMN and Quantum mechanics. Quím Nova 40:774–780. https://doi.org/10.21577/0100-4042.20170059

Pikkemaat MG, Linssen AB, Berendsen HJ, Janssen DB (2002) Molecular dynamics simulations as a tool for improving protein stability. Protein Eng 15(3):185–192. https://doi.org/10.1093/protein/15.3

Plotino G, Grande NM, Mercade M (2019) Photodynamic therapy in endodontics. Int Endod J 52(6):760–774. https://doi.org/10.1111/iej.13057
Polat E, Kang K (2021) Natural photosensitizers in Antimicrobial Photodynamic Therapy. Biomedicines 9(6):584. https://doi.org/10.3390/biomedicines9060584
Pourhajibagher M, Bahador A (2024) Bioinformatics analysis of photoexcited natural flavonoid glycosides as the inhibitors for oropharyngeal HPV oncoproteins. AMB Express 14(1):29. https://doi.org/10.1186/s13568-024-01684-6
Pourhajibagher M, Chiniforush N, Raoofian R, Pourakbari B, Ghorbanzadeh R, Bazarjani F, Bahador A (2016) Evaluation of photo-activated disinfection effectiveness with methylene blue against Porphyromonas gingivalis involved in endodontic infection: an in vitro study. Photodiagnosis Photodyn Ther 16:132–135. https://doi.org/10.1016/j.pdpdt.2016.09.008
Pourhajibagher M, Alaeddini M, Etemad-Moghadam S, Parker S, Bahador A (2023a) Effects of Kojic Acid-mediated Sonodynamic Therapy as a Matrix Metalloprotease-9 inhibitor against oral squamous cell carcinoma: a Bioinformatics Screening and in vitro analysis. Curr Drug Discov Technol 1–10. https://doi.org/10.2174/0115701638266082231124055825
Pourhajibagher M, Azimi Mohammadabadi M, Ghafari HA, Hodjat M, Bahador A (2023b) Evaluation of anti-biofilm effect of antimicrobial sonodynamic therapy-based periodontal ligament stem cell-derived exosome-loaded kojic acid on *Enterococcus faecalis* biofilm. J Med Microbiol 72(11):001772. https://doi.org/10.1099/jmm.0.001772
Rao VS, Srinivas K, Sujini GN, Kumar GN (2014) Protein-protein interaction detection: methods and analysis. Int J Proteom 2014:147648. https://doi.org/10.1155/2014/147648
Ribeiro M, Gomes IB, Saavedra MJ, Simões M (2022) Photodynamic therapy and combinatory treatments for the control of biofilm-associated infections. Lett Appl Microbiol 75(3):548–564. https://doi.org/10.1111/lam.13762
Salsbury FR Jr Molecular dynamics simulations of protein dynamics and their relevance to drug discovery (2010). Curr Opin Pharmacol 10(6):738–744. https://doi.org/10.1016/j.coph.2010.09.016
Sankararaman S, Sha F, Kirsch JF, Jordan MI, Sjölander K (2010) Active site prediction using evolutionary and structural information. Bioinformatics 26(5):617–624. https://doi.org/10.1093/bioinformatics/btq008
Schmittgen TD, Livak KJ (2008) Analyzing real-time PCR data by the comparative C(T) method. Nat Protoc 3(6):1101–1108. https://doi.org/10.1038/nprot.2008.73
Schneewind O, Missiakas D (2014) Sec-secretion and sortase-mediated anchoring of proteins in Gram-positive bacteria. Biochim Biophys Acta 1843(8):1687–1697. https://doi.org/10.1016/j.bbamcr.2013.11.009
Segura-Egea JJ, Martín-González J (2020) Endodontic Emergencies and Systemic Antibiotics in Endodontics. Endodontic Advances and Evidence-Based Clinical Guidelines 734–48. https://doi.org/10.1002/9781119553939.ch28
Toledo-Arana A, Valle J, Solano C, Arrizubieta MJ, Cucarella C, Lamata M, Amorena B, Leiva J, Penadés JR, Lasa I (2001) The enterococcal surface protein, Esp, is involved in *Enterococcus faecalis* biofilm formation. Appl Environ Microbiol 67(10):4538–4545. https://doi.org/10.1128/AEM.67.10.4538-4545.2001
Sevimoglu T, Arga KY (2014) The role of protein interaction networks in systems biomedicine. Comput Struct Biotechnol J 11(18):22–27. https://doi.org/10.1016/j.csbj.2014.08.008
Shaker B, Ahmad S, Lee J, Jung C, Na D (2021) In silico methods and tools for drug discovery. Comput Biol Med 137:104851. https://doi.org/10.1016/j.compbiomed.2021.104851
Sinha S, Tam B, Wang SM (2022) Applications of Molecular Dynamics Simulation in protein study. Membr (Basel) 12(9):844. https://doi.org/10.3390/membranes12090844
Tseng TT, Tyler BM, Setubal JC (2009) Protein secretion systems in bacterial-host associations, and their description in the Gene Ontology. BMC Microbiol 9(Suppl 1):S2. https://doi.org/10.1186/1471-2180-9-S1-S2
Tsirigotaki A, De Geyter J, Šoštaric N, Economou A, Karamanou S (2017) Protein export through the bacterial sec pathway. Nat Rev Microbiol 15(1):21–36. https://doi.org/10.1038/nrmicro.2016.161
van Wely KH, Swaving J, Freudl R, Driessen AJ (2001) Translocation of proteins across the cell envelope of Gram-positive bacteria. FEMS Microbiol Rev 25(4):437–454. https://doi.org/10.1111/j.1574-6976.2001.tb00586.x
Voit M, Trampuz A, Gonzalez Moreno M (2022) In Vitro evaluation of five newly isolated bacteriophages against *E. Faecalis* Biofilm for their potential use against post-treatment apical periodontitis. Pharmaceutics 14(9):1779. https://doi.org/10.3390/pharmaceutics14091779
Weinstein JY, Martí-Gómez C, Lipsh-Sokolik R, Hoch SY, Liebermann D, Nevo R, Weissman H, Petrovich-Kopitman E, Margulies D, Ivankov D, McCandlish DM, Fleishman SJ (2023) Designed active-site library reveals thousands of functional GFP variants. Nat Commun 14(1):2890. https://doi.org/10.1038/s41467-023-38099-z
Zilles JC, Dos Santos FL, Kulkamp-Guerreiro IC, Contri RV (2022) Biological activities and safety data of kojic acid and its derivatives: a review. Exp Dermatol 31(10):1500–1521. https://doi.org/10.1111/exd.14662
Zoletti GO, Siqueira JF Jr, Santos KR (2006) Identification of *Enterococcus faecalis* in root-filled teeth with or without periradicular lesions by culture-dependent and-independent approaches. J Endod 32(8):722–726. https://doi.org/10.1016/j.joen.2006.02.001
Zoletti GO, Pereira EM, Schuenck RP, Teixeira LM, Siqueira JF Jr, dos Santos KR (2011) Characterization of virulence factors and clonal diversity of *Enterococcus faecalis* isolates from treated dental root canals. Res Microbiol 162(2):151–158. https://doi.org/10.1016/j.resmic.2010.09.018

Publisher's note